buildings

MDPI

Article

Utilization of High-Performance Concrete Mixtures for Advanced Manufacturing Technologies

Oldrich Sucharda, Radoslav Gandel *, Petr Cmiel, Jan Jerabek and Vlastimil Bilek

Department of Building Materials and Diagnostics of Structures, Faculty of Civil Engineering, VSB—Technical University of Ostrava, Ludvika Podeste 1875/17, 708 00 Ostrava-Poruba, Czech Republic; oldrich.sucharda@vsb.cz (O.S.); petr.cmiel@vsb.cz (P.C.); jan.jerabek@vsb.cz (J.J.); vlastimil.bilek@vsb.cz (V.B.)
* Correspondence: radoslav.gandel@vsb.cz

Abstract: The presented experimental program focuses on the design of high-performance dry concrete mixtures, which could find application in advanced manufacturing technologies, for example, additive solutions. The combination of high-performance concrete (HPC) with advanced or additive technologies provides new possibilities for constructing architecturally attractive buildings with high material requirements. The purpose of this study was to develop a dry mixture made from high-performance concrete that could be distributed directly in advanced or additive technologies of solutions in pre-prepared condition with all input materials (except for water) in order to reduce both financial and labor costs. This research specifically aimed to improve the basic strength characteristics—including mechanical (assessed using compressive strength, tensile splitting strength, and flexural strength tests) and durability properties (assessed using tests of resistance to frost, water, and defrosting chemicals)—of hardened mixtures, with partial insight into the rheology of fresh mixtures (consistency as assessed using the slump-flow test). Additionally, the load-bearing capacity of the selected mixtures in the form of specimens with concrete reinforcement was tested using a three-point bending test. A reference mixture with two liquid plasticizers—the first based on polycarboxylate and polyphosphonate and the second based on polyether carboxylate—was modified using a powdered plasticizer based on the polymerization product Glycol to create a dry mixture; the reference mixture was compared with the developed mixtures with respect to the above-mentioned properties. In general, the results show that the replacement of the aforementioned liquid plasticizers by a powdered plasticizer based on the polymerization product Glycol in the given mixtures is effective up to 5% (of the cement content) with regard to the mechanical and durability properties. The presented work provides an overview of the compared characteristics, which will serve as a basis for future research into the development of additive manufacturing technologies in the conditions of the Czech Republic while respecting the principles of sustainable construction.

Keywords: high-performance concrete; dry concrete mixtures; advanced manufacturing technologies; mechanical properties; durability; experiment

check for updates

Citation: Sucharda, O.; Gandel, R.; Cmiel, P.; Jerabek, J.; Bilek, V. Utilization of High-Performance Concrete Mixtures for Advanced Manufacturing Technologies. *Buildings* **2024**, *14*, 2269. https://doi.org/10.3390/buildings14082269

Academic Editors: Kamila Kotrasová, Dušan Katunský, Martina Zeleňáková and Peter Mésároš

Received: 25 April 2024
Revised: 12 July 2024
Accepted: 15 July 2024
Published: 23 July 2024

Copyright: © 2024 by the authors. Licensee MDPI, Basel, Switzerland. This article is an open access article distributed under the terms and conditions of the Creative Commons Attribution (CC BY) license (https://creativecommons.org/licenses/by/4.0/).

1. Introduction

The importance of concrete as a building material is irreplaceable. It finds application in all construction and structural parts of buildings, where the key research topics include the use of advanced technologies while respecting sustainable construction and a circular economy. From the point of view of materials engineering, this includes the use of HPC concrete, which brings significantly better mechanical properties, improved durability, and technological solution possibilities. For example, the above is connected with the advanced use of 3D printing and advanced technology for the creation of sophisticated formwork solutions, shells, and composite structures based on multiple material solution variants. In these cases, HPC concretes are advantageous because they are self-compacting and have excellent workability. Other possibilities include the very use of additive manufacturing of

concrete (AMoC). AMoC is a term that refers to a set of activities leading to the creation of three-dimensional objects using digital models [1,2].

A simplified yet very precise term for additive concrete manufacturing is 3D concrete printing (3DCP). The most widespread method of 3D printing is considered to be one where fresh concrete is extruded from a nozzle, forming a rising layered product [3–5]. Extrusion is ensured by continuously pumping fresh concrete, and individual layers maintain the printed shape even when subjected to simultaneous loading by subsequent layers without the use of formwork [6–8]. Although this technology has been under research for several years and has already produced simple-to-relatively complex building elements and structures [9–15], it is still in its infancy.

Currently, there is an urgency to reduce the amount of raw materials used since the construction industry generates a significant share of CO_2 emissions in the atmosphere [16,17]. Furthermore, with conventional concrete technology, geometric simplicity is chosen at the expense of an optimized volume of concrete. In simpler terms, utilizing 3D printing is beneficial because it helps reduce the amount of concrete needed while also optimizing the use of raw materials [18–20].

There are several application technologies for additive manufacturing processes. For example, in his research, Chuang [21] describes one of the first additive manufacturing technologies—SL photopolymerization—for printing LRS paste consisting of CUG-1A powder, which has similar properties to lunar regolith from the Apollo14 sampling site. SLA uses a UV laser to cure photopolymer resin. The laser traces each layer of the object in the liquid resin, solidifying it and bonding it to the layer below.

With the advancement of 3D concrete printing technologies, experimentation with alternative materials is gradually emerging. In continuation of previous research, which primarily focused on the mechanical and durability properties of hardened mixtures, such as high-performance concretes [22,23], fiber-reinforced concretes [24], alkali-activated materials [25–27], or hybrid composites [28], it is necessary to thoroughly examine the relationship between pumpability, extrudability, and workability. The curing of 3D-printed concrete also plays an important role in its resulting properties. Xiaofei [29], in his publication, for example, discusses the advantages and disadvantages of steam-cured 3D-extruded concrete, among other issues.

For illustration, in Figure 1, it is possible to see individual typical aspects of the development of a concrete mixture for additive technologies from the point of view of materials engineering, including the possibility of printing individual layers on top of each other, the height of the printing layer, the workability time, the visual aspects of the concrete mixture, and the mechanical properties with regard to workability. Figure 1 illustrates the initial phase of the author's research work in the development of the mixture in the laboratory.

Many researchers have explored alternative materials for 3D printing. For example, Gökçe [30] and Qaidi [31] critically evaluated the potential use of geopolymers in 3D printing in their studies. On the other hand, Mengistu [32] investigated the utilization of waste concrete from 3D printing as recycled aggregate for new 3D concrete printing. The exploration of using fiber-reinforced concrete in 3D printing has not avoided the use of fiber concrete altogether. This composite material encompasses a wide range of combinations of concrete with various types of fibers, which differ in the type of material, size, and shape and have diverse properties. Ungureanu [33] observed the behavior of fiber–concrete mixtures composed of Portland slag cement CEM II/AS 52.5 R and reinforced with polypropylene fibers with a length of 12 mm and a diameter of 21–34 μm in both fresh and hardened states. Li [34] compared the properties of 3D-printed samples made of cementitious mortar reinforced with carbon fibers at various proportions with those of conventionally cast concrete samples. Arunothayan [35] went a step further and, in his experimental program, combined 3D printing of concrete with ultra-high-performance concrete reinforced with steel fibers.

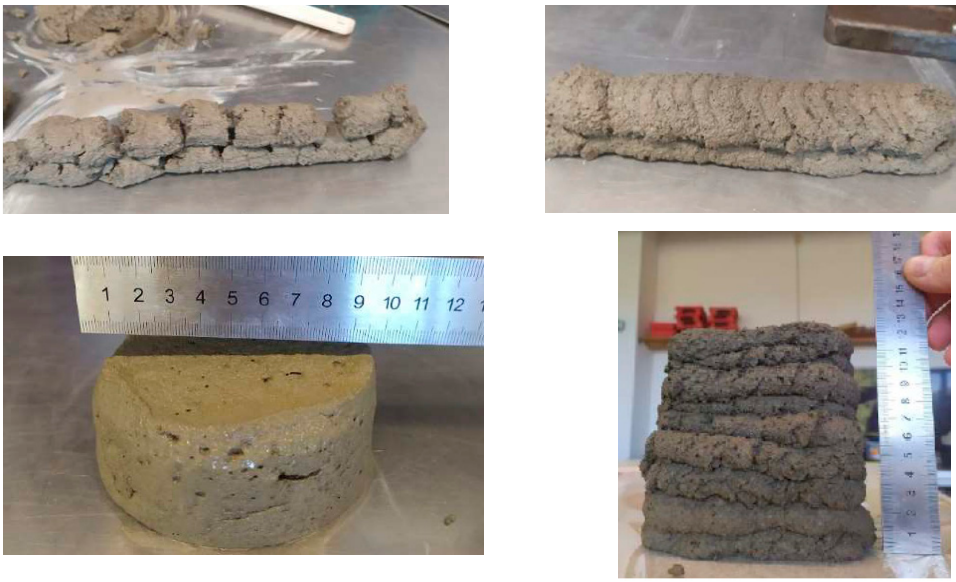


Figure 1. Initial phase of concrete mixture development for additive technologies in the laboratory.

High-performance concrete is an innovative material that offers a range of advantages over ordinary concrete. A major advantage of it is its high strength and resistance to mechanical loading. A finer aggregate fraction, together with high-strength cement and the presence of silica fume, creates a denser and less porous structure that is resistant to water penetration into the structural elements, which has been associated with many degradation processes. This compensates for its higher purchase price since the costs for additional maintenance and repairs throughout its entire lifespan are comparably smaller than those of ordinary concrete. A quality selection of raw materials and a more demanding technological process in production and application will, thus, pay off over the years.

In addition to the above-mentioned research, other studies have also investigated the use of high-performance concrete in 3D printing [36–38]. Apart from examining the required strength and durability characteristics of the resulting hardened products and the ratio between the pumpability, extrudability, and workability of fresh mixtures, it is also necessary to focus on the development of mixtures that, in the event of practical expansion, could be prepared in such a way as to maximize ease for users during their subsequent preparation. Table 1 summarizes the basic attributes of 3D-extruded concrete.

Table 1. Attributes of 3D-printed concrete.

Attribute	Description
Rheology	Flow properties important for pumpability and extrudability
Printability	Ability to be extruded and maintain shape
Buildability	Capacity to support subsequent layers
Strength characteristics	Ability to withstand loads
Bond strength	Adhesion between layers
Durability	Long-term performance under environmental conditions

In the context of 3D-printed high-strength concrete, the attributes listed in Table 1 have been addressed in several studies. For example, Le [39] observed the properties of a fresh mixture, such as extrudability, buildability, and workability, using samples of 3D-printed high-performance concrete reinforced with polypropylene fibers. Based on the results, the author utilized the mixture and tested it on real structural elements. Aside from the strength characteristics of hardened 3D-printed concrete, the bond strength between layers is also important. Wolf [40] and Sanjayan [41] examined the dependence of several factors on the bond strength of the interlayer, such as the interlayer interval time, the height of

the nozzle, and the moisture level between layers, which exerts a great influence on the resulting strength characteristics and durability of the extruded 3D element.

The aim of the present research task, an experimental program [42], was to create a dry mixture of HPC with all the necessary input raw materials (excluding water). Such a mixture could ideally be distributed in a pre-prepared state. The area of application is primarily in advanced technological solutions, which also includes the area of additive technologies. The experimental program was designed to primarily focus on the strength, including the mechanical and durability properties, of hardened HPC mixtures with the substitution of liquid plasticizers by a powdered plasticizer. This work investigated the rheology of fresh mixtures only marginally.

2. Materials and Methods

2.1. Mixture Development

The selected reference mixture for HPC and the experimental program served as a starting point [42,43]. The mixture design in this case involved replacing the original chemical ingredients. The reference mixture (REF) included two liquid plasticizers based on polycarboxylate, polyphosphonate, and polyether carboxylate. These additives were replaced by a single powdered superplasticizer based on the polymerization product Glycol to develop a different mixture [44–46].

The powdered plasticizer used in this study is intended to be dosed according to the recommendations in the technical datasheet, ranging from 2% to 5% of the cement weight. For the purpose of this study, quantities of 3%, 4%, and 5% were chosen. Alongside the reference mixture, four different mixtures were tested, which were labeled as follows: REF, MEL03, MEL04, and MEL05. Table 2 lists the dosages of individual ingredients per 1 m^3 of concrete mix.

Table 2. HPC mixture designs.

REF Mixture		**MEL 03 Mixture**		**MEL 04 Mixture**		**MEL 05 Mixture**	
Input materials	Weight per 1 m^3	Input materials	Weight per 1 m^3	Input materials	Weight per 1 m^3	Input materials	Weight per 1 m^3
Cement 42.5 R	650	Cement 42.5 R	650	Cement 42.5 R	650	Cement 42.5 R	650
Water	150	Water	150	Water	150	Water	150
Tovacov aggregate: 0–4 mm	890	Tovacov aggregate: 0–4 mm	890	Tovacov aggregate: 0–4 mm	890	Tovacov aggregate: 0–4 mm	890
Litice aggregate: 4–8 mm	570	Litice aggregate: 4–8 mm	570	Litice aggregate: 4–8 mm	570	Litice aggregate: 4–8 mm	570
Limestone: finely ground	80	Limestone: finely ground, roughness of 8	80	Limestone: finely ground, roughness of 8	80	Limestone: finely ground, roughness of 8	80
Silica fume	70	Silica fume	70	Silica fume	70	Silica fume	70
(Polyether carboxylate) plasticizer	20	(Glycol) plasticizer	19.5	(Glycol) plasticizer	26	(Glycol) plasticizer	32.5
(Polycarboxylate and polyphosphonate) plasticizer	10						

At the same time, during the selection of raw materials for the concrete mixture, a study of the individual components of the recipe was carried out. In the case of the Tovacov aggregate (0–4 mm) and the Litice aggregate (4–8 mm), a classic Particle Size Distribution

(PSD) using test sieves was performed. In both cases, the aggregate suppliers declare their suitability for use in concrete mixtures. The test results are depicted in Figures 2 and 3.

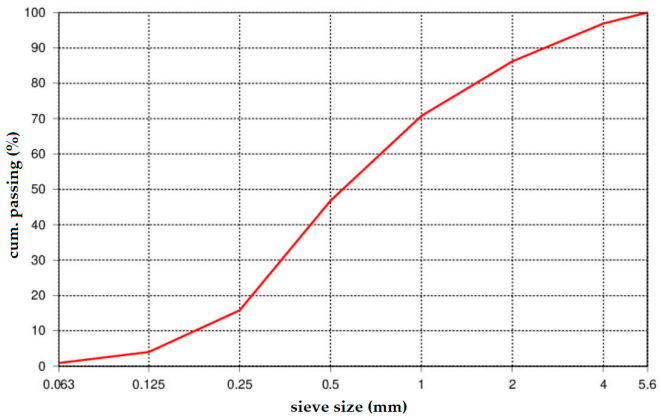


Figure 2. Tovacov aggregate (0–4 mm)—granularity.

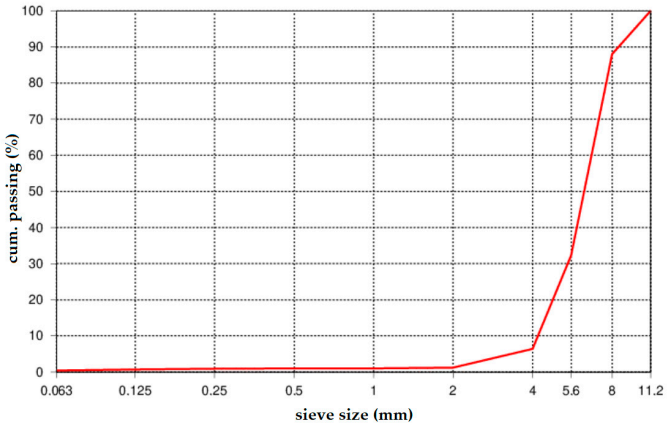
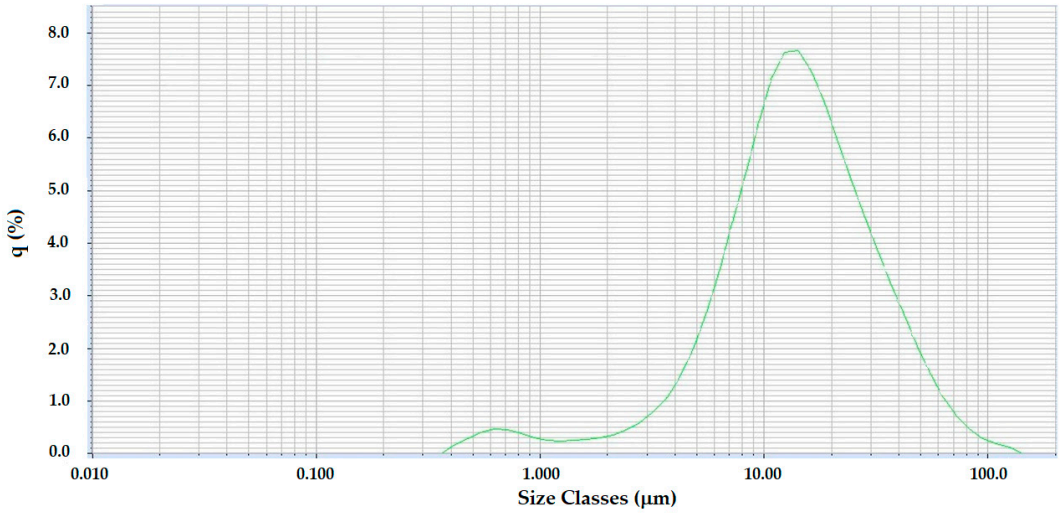


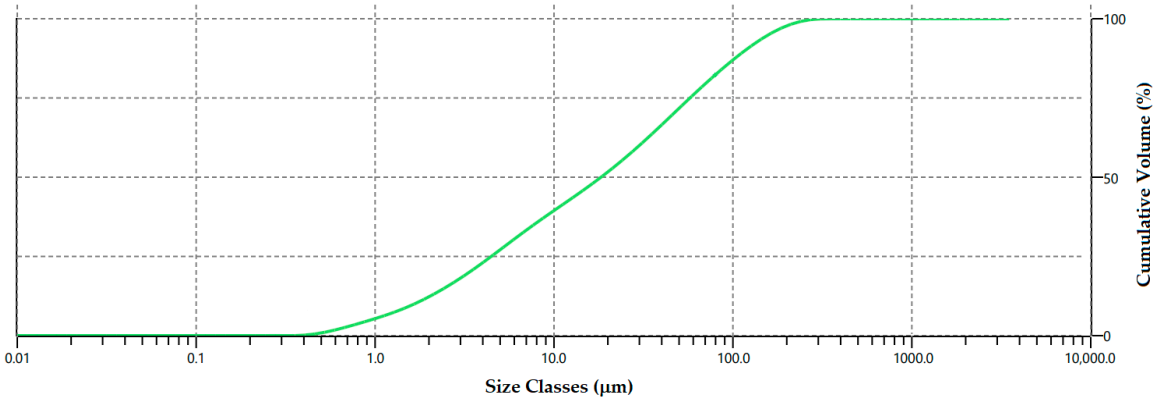
Figure 3. Litice aggregate (4–8 mm)—granularity.

In the case of cement, the laser diffraction particle size analyzer from the HORIBA (Kyoto, Japan) LA series was used with regard to particle size. A variant of the dry route was used, and the measurement data have been processed in the form of Figure 4a. The main characterization of the particle size result is D(v, 0.5)—median size, which was 14.01829 µm. The results are in the expected range. In the case of limestone and silica fume, the laser granulometer manufactured by MalvernPanalytical (Malvern, UK) (Mastersizer 3000) was used to measure the particle size when the wet path in water was used. In the case of limestone, the range of the measured particle sizes was larger than in the case of silica fume. In this case, the results are expressed as cumulative volume (%) in Figure 4b for limestone and in Figure 4c for silica fume. In both cases, the values are again within the expected range. The measurements carried out were of an informative nature regarding with aspect the capacity options of the measuring devices and labs; the mentioned measurements were followed by the characterization of the particles with a microscope.

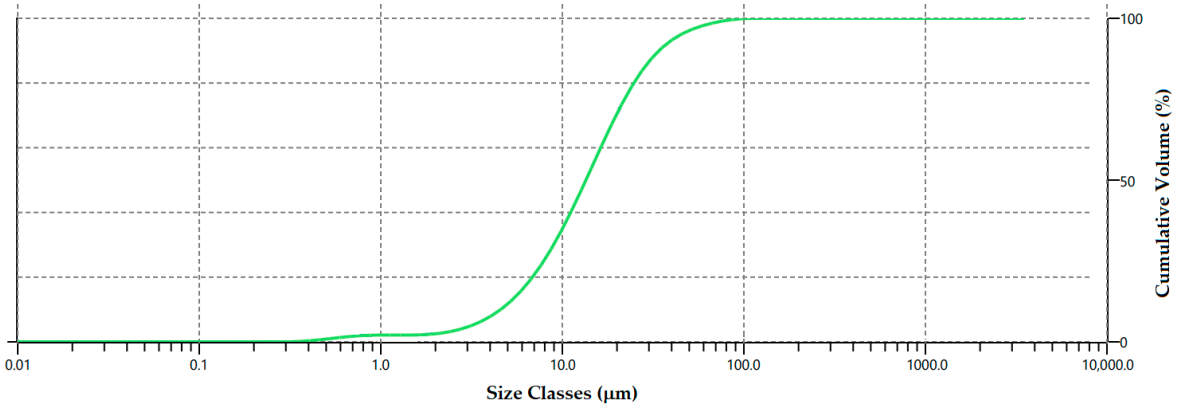
Furthermore, for the characterization of the main and additional components of the recipe, a digital microscope with a high resolution of 4 K was used to verify the size and shape; a resolution from 20× to 2000× was used. The measurement results are shown in Figure 5, where a legend with a magnification scale is given for each sub-figure (Figure 5a–f).



(**a**) Cement 42.5 R

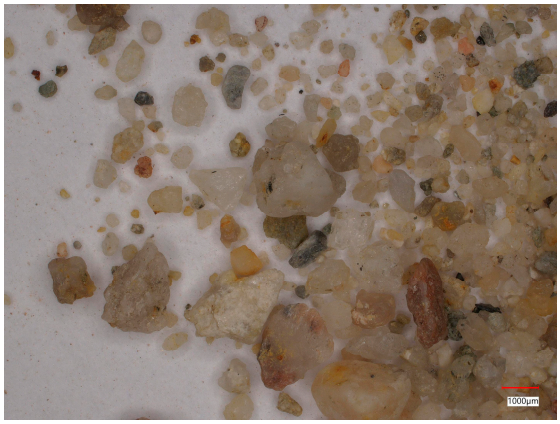


(**b**) Limestone

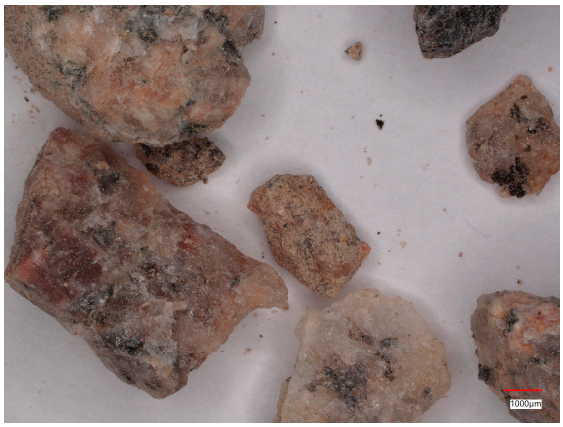


(**c**) Silica fume

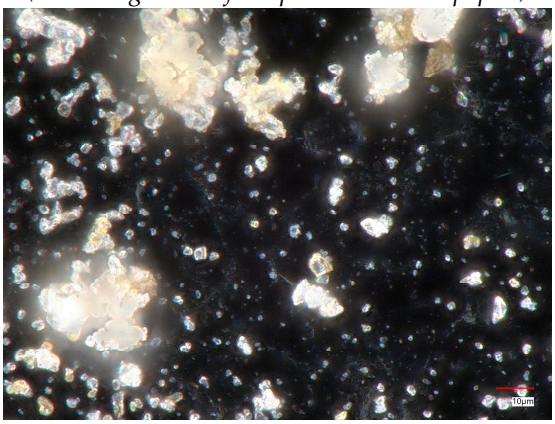
Figure 4. Particle size analysis. (**a**) Cement 42.5—q (%); (**b**) limestone—cumulative volume (%); (**c**) silica fume—cumulative volume (%).



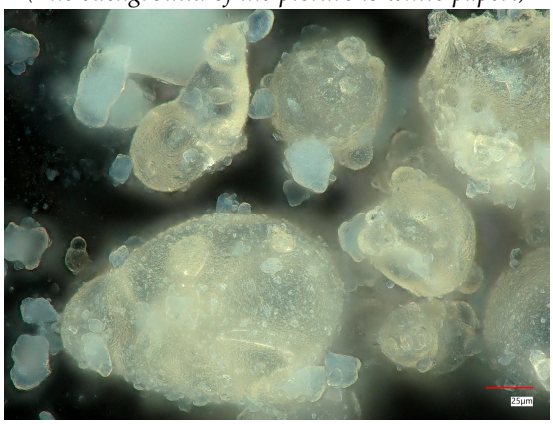
(**a**) Tovacov aggregate (0–4 mm)
Zoom 20×, red line is 1000 µm
(The background of the picture is white paper.)



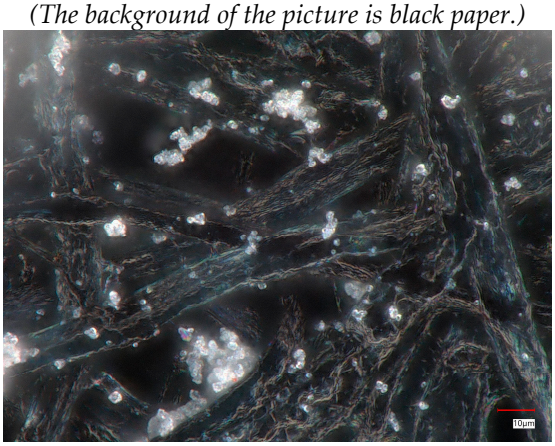
(**b**) Litice aggregate (4–8 mm)
Zoom 20×, red line is 1000 µm
(The background of the picture is white paper.)



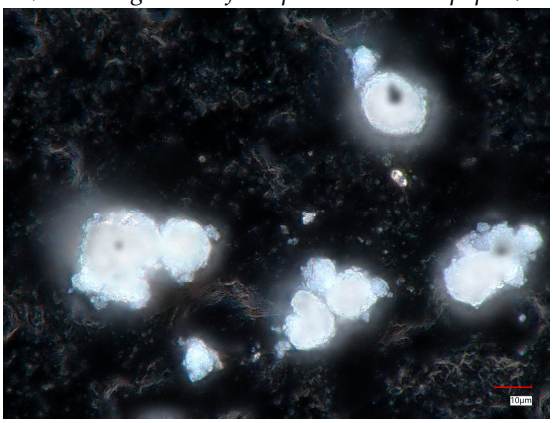
(**c**) Cement 42.5 R
Zoom 2000×, red line is 10 µm
(The background of the picture is black paper.)



(**d**) Plasticizer
Zoom 1000×, red line is 25 µm
(The background of the picture is black paper.)



(**e**) Limestone
Zoom 2000×, red line is 10 µm
(The background of the picture is black paper.)



(**f**) Silica fume
Zoom 2000×, red line is 10 µm
(The background of the picture is black paper.)

Figure 5. Aggregates and concrete mix particles: (**a**) Tovacov aggregate (0–4 mm); (**b**) Litice aggregate (4–8 mm); (**c**) cement 42.5 R; (**d**) plasticizer; (**e**) limestone; (**f**) silica fume.

2.2. Determination of Consistency Using Mini-Cone Flow Test

This test was conducted according to the ČSN EN 1015-3 standard [44], with the following modification: a stainless-steel table was used instead of the specified baseplate. The poured concrete was measured in two perpendicular directions, and the diameter was

calculated from these two measurements. Based on the obtained value of the spill diameter of the mini-cone and the consistency of the fresh mixtures, the mixtures were subsequently classified according to the TP 07 [45] technical regulation into individual categories. Table 3 shows a comparison of two mixtures during the flow test.

Table 3. Classification of the mixtures according to the spread of the mini-cone.

Mixture	Average Spread [mm]	Classification According to TP 07
REF	260	K2 Viscous
Mel 03	180	K3 Thixotropic
Mel 04	200	K3 Thixotropic
Mel 05	210	K3 Thixotropic

2.3. Determination of the Bulk Density of Hardened Concrete

The bulk density was determined experimentally on 19 specimens for each mixture. Figure 6 shows the results, including the respective statistical characteristics.

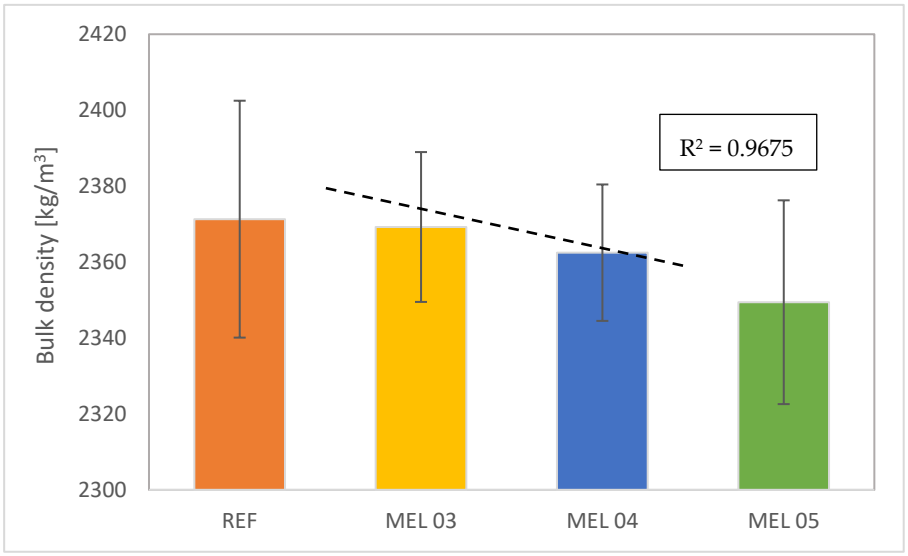


Figure 6. Average bulk density of the tested mixtures (dotted line—trend line).

From the bar chart in Figure 6, it is obvious that the samples from the reference mixture achieved the highest bulk densities. The average bulk density values of the mixtures containing the powdered plasticizer decreased almost directly proportionally (coefficient of determination R^2 = 96.75%) with an increasing dosage of the mentioned plasticizer. With an increasing content of the powdered plasticizer, the air content increased, resulting in an almost linear decrease in bulk density. This was evident in the number of pores present in the samples of the individual mixtures.

2.4. Strength Characteristics

2.4.1. Compressive Strength

Compressive strength was tested in accordance with the ČSN EN 12390-3 standard [46] on cubes with an edge length of 100 mm and the ČSN EN 196-1 standard [47] on fractured specimens of beam fragments with dimensions of 40 × 40 × 160 mm; the latter constituted a non-compliance with the standard as the tested specimens were not cement beams. For each mixture, 6 values were determined for the 7-day compressive strength, 12 values for the 28-day strength, and 6 values for the 56-day strength using the beam fragments; in addition, seven cubes were tested for the standard 28-day compressive strength. The corresponding strength characteristics are shown in bar charts in Figures 7 and 8.

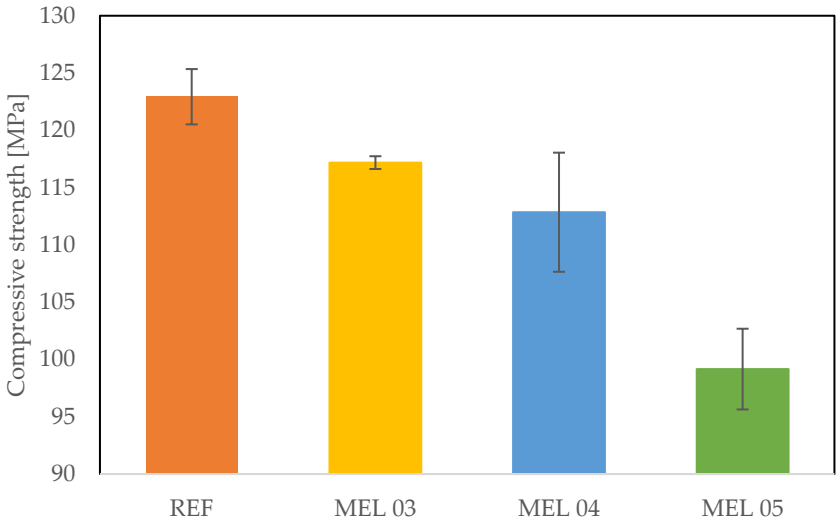


Figure 7. Illustration of 28-day compressive strength of the tested mixtures on cubes with a 100 mm edge length.

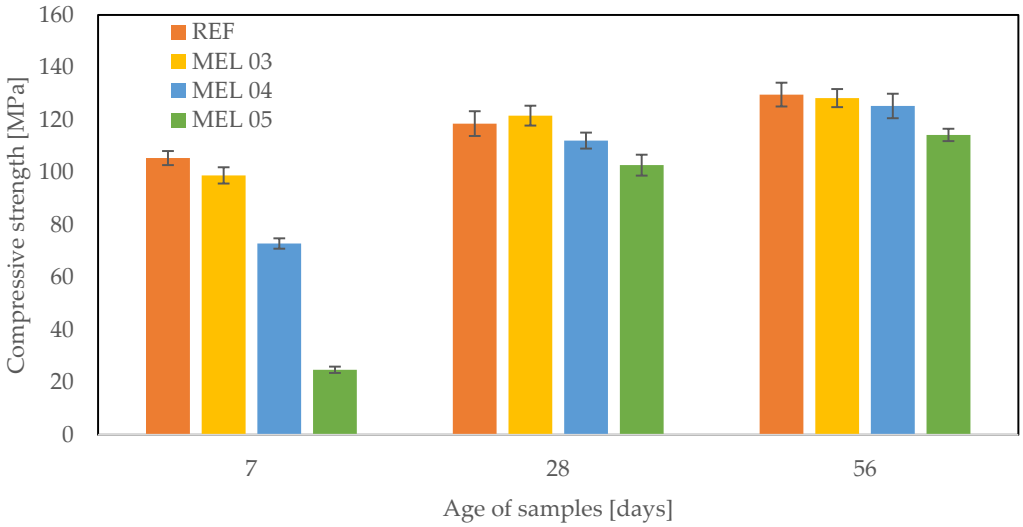


Figure 8. Development of compressive strength over time on beam fragments with dimensions of 40 × 40 × 160 mm.

As shown in Figures 7 and 8, the average compressive strength decreases with an increasing content of the powdered plasticizer compared to the reference mixture with liquid plasticizers. The MEL 03 mixture is the closest to the reference mixture in terms of compressive strength. In Figure 8, there is also a clear change in compressive strength over time, depending on the dosage of the powdered plasticizer. In the case of the MEL 05 mixture, a significantly lower 7-day compressive strength (approx. 25 MPa) was observed compared to the other mixtures. It is necessary to mention that an increased amount of powdered plasticizer has a negative effect on the maturation of the mixtures, which is reflected by a lower increase in initial compressive strength in the first 7 days. After the standard period of 28 days, the strength characteristics increase and stabilize.

2.4.2. Tensile Splitting Strength

Tensile splitting strength was tested in accordance with the ČSN EN 12390-6 standard [48] on six concrete cube samples with an edge length of 150 mm. The test specimens were positioned (see Figure 9) so that the jaws of the press acted perpendicular to the direction of filling. The loading rate of the specimens was 0.04–0.06 MPa/s until failure

occurred. Based on the achieved maximum load force, the tensile splitting strength was subsequently determined according to the relevant standard [48].

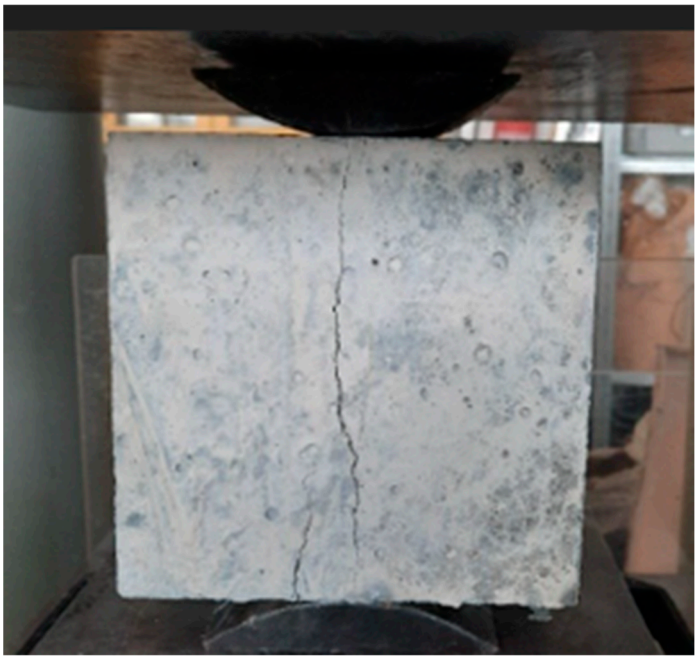


Figure 9. Crack on a sample after tensile splitting strength test.

The test results are summarized in Figure 10, which provides the descriptive statistics of the strength values of all the tested mixtures.

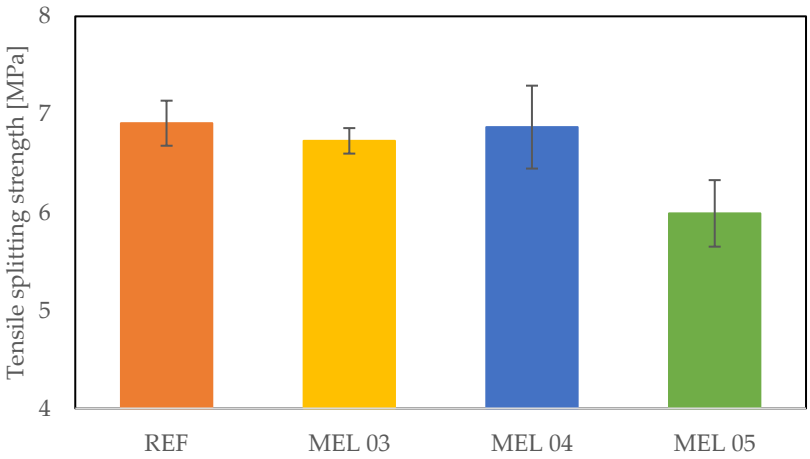


Figure 10. Illustration of 28-day tensile splitting strength of the tested mixtures on cubes with a 150 mm edge length.

From Figure 10, it can be concluded, once again, that with an increasing content of the powdered plasticizer, the tensile splitting strength decreases. In this case, the average value of the observed tensile splitting strength of the MEL 04 mixture (6.87 MPa) exceeded that of the MEL 03 mixture (6.73 MPa) and approached that of the reference mixture (6.91 MPa). This is likely due to the high variability in the values of tensile splitting strength obtained during the test. The values of the REF, MEL 03, and MEL 04 mixtures are relatively similar; thus, it is clear that the critical amount of powdered plasticizer that affects mechanical properties ranges from 5% upwards.

2.4.3. Flexural Strength

Flexural strength was tested according to the ČSN EN 12390-5 standard [49] on beams with dimensions of 40 × 40 × 160 mm. The specimens were placed in the press so that the direction of loading was perpendicular to the direction of filling. From the obtained maximum force, flexural strength was again calculated according to the standard [49].

The respective results are provided in Figure 11.

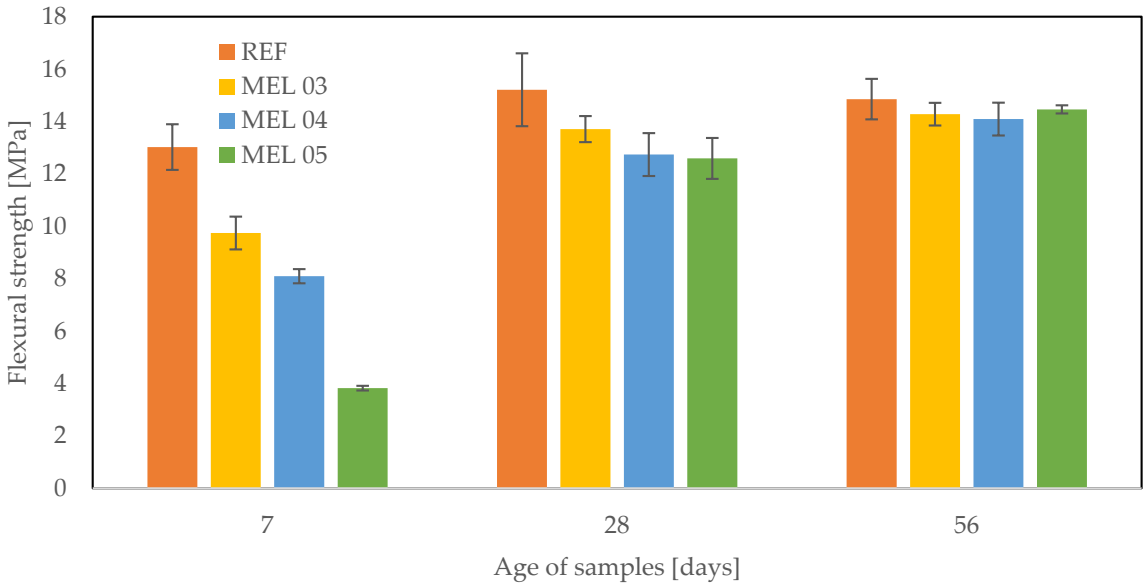


Figure 11. Development of flexural strength over time on beams with dimensions of 40 × 40 × 160 mm.

The flexural strength of the samples at the age of 7 days decreased with a higher content of powdered plasticizer, with the highest values exhibited by the reference mixture at 13 MPa.

At the age of 28 days, flexural strength also decreased with a higher content of powdered plasticizer, although this decrease in strength was not as significant compared with the samples at the age of 7 days. The highest strength was again exhibited by the reference mixture (15.2 MPa).

In the case of flexural strength at the age of 56 days, it seems that all mixtures with the powdered plasticizer achieved comparable values. The highest flexural strength was again exhibited by the reference mixture at 14.9 MPa (although with a slight decrease of 0.3 MPa compared to the 28-day flexural strength), and the lowest strength was exhibited by the MEL 04 mixture at 14.1 MPa.

Based on these results, it is evident that, despite the relatively high variability in flexural strength in the initial days, relatively stable similar values were observed for all mixtures after reaching an age of approximately 2 months. An increased amount of powdered plasticizer adversely affected the setting and hardening time of the mixtures, which manifested as a lower increase in the initial flexural strength (7 days). After the standard period (28 days), the strength characteristics increased and stabilized. However, the measured flexural strength values for the samples containing the powdered plasticizer did not reach the value of the reference mixture.

2.5. Resistance of Cement Concrete Surface to Water and Defrosting Chemicals

Resistance to water and defrosting chemicals was tested with deviations from the ČSN 73 1326 standard [50]. One difference lied in the arrangement of the test specimens (with an edge length of 100 mm) so that the surface in contact with the salt solution was also in contact with the bottom of the testing dish. This measure was implemented because of the segregated layer created on the surface of some mixtures containing the powdered

plasticizer. In Figure 12, a cube of the MEL 05 mixture for example from experimental program. Another difference was the number of cycles, which increased due to the higher expected resistance to water and defrosting chemicals.

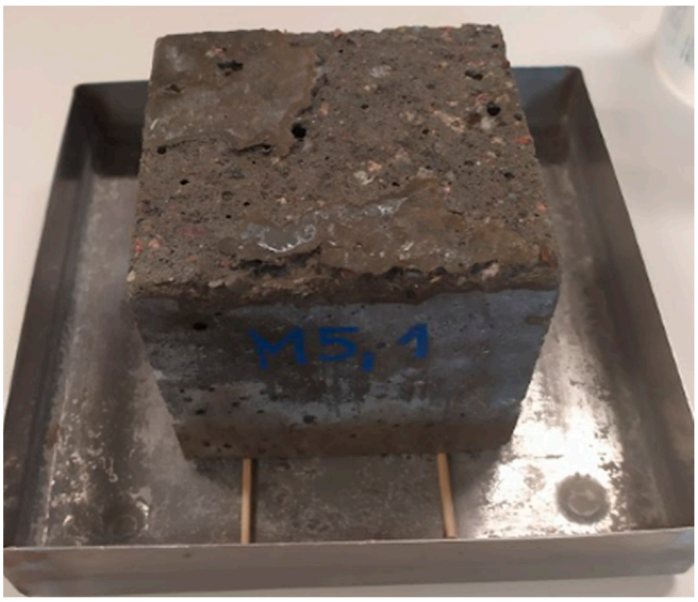


Figure 12. Mass loss on a cube sample of the MEL 05 mixture.

The graphical visualization of total waste amount after a number of individual cycles for the REF, MEL 03, and MEL 04 mixtures is presented in Figure 13, while the visualization for the MEL 05 mixture is shown in Figure 14. This was performed to obtain a clearer picture of the results influenced by the comparatively higher waste values of the MEL 05 mixture. The waste values with their corresponding statistical characteristics are displayed in Figures 13 and 14.

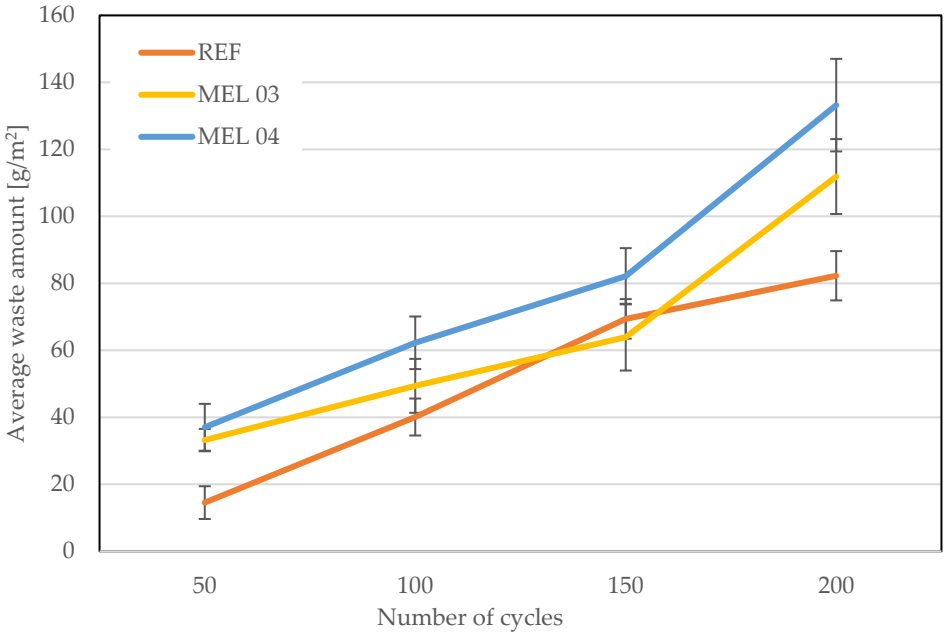


Figure 13. Comparison of overall average waste after a number of individual cycles for the REF, MEL 03, and MEL 04 mixtures.

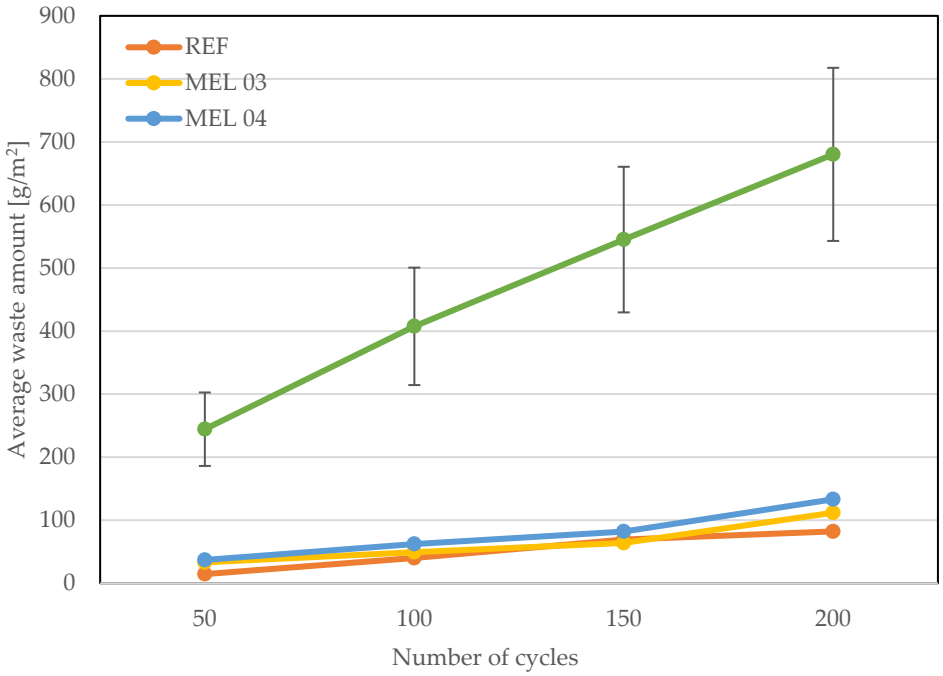


Figure 14. Total waste of the MEL 05 mixture compared with the values of the REF, MEL 03, and MEL 04 mixtures.

By comparing the graphical visualization of the waste amounts of individual mixtures in Figures 13 and 14, it can be concluded that the amount of powdered plasticizer affects the mixtures' resistance to water and defrosting chemicals. With an increasing amount of powdered plasticizer, the resistance to water and defrosting chemicals decreases. The REF mixture displayed the highest resistance, closely followed by the MEL 03 and MEL 04 mixtures. The MEL 05 mixture showed significantly lower resistance to water and defrosting chemicals than the other mixtures (due to its more porous structure). From the perspective of categorization based on resistance to water and defrosting chemicals according to the ČSN 73 1326 standard [50] after 200 cycles, the REF, MEL 03, and MEL 04 mixtures belong to category 2 (slightly damaged; total waste < 500 g/m^2), and the MEL 05 mixture belongs to category 3 (damaged; total waste < 1000 g/m^2). Figure 14 also visually compares the quantity of waste of the MEL 05 mixture with the remaining mixtures.

2.6. Dynamic Modulus of Elasticity

The determination of the dynamic modulus of elasticity using ultrasonic testing was performed in accordance with the ČSN 73 1371 standard [51] on beams with dimensions of 40 × 40 × 160 mm. The dynamic modulus of elasticity was compared between seven reference samples aged 28 days and seven samples that were aged 28 days and had undergone 200 freezing cycles. Figure 15 shows the average results of the dynamic modulus of elasticity for the reference and frozen samples.

From Figure 15, it is evident that the dynamic modulus of elasticity was reduced for the majority of specimens that underwent freezing cycles. An exception could be observed for the MEL 03 mixture, which may be attributed to human error or the small statistical dataset. A significant decrease in the dynamic modulus was observed for the MEL 05 mixture, with higher variance in values compared to other mixtures, which was caused by the more noticeable disruption of the sample structure compared to the other mixtures.

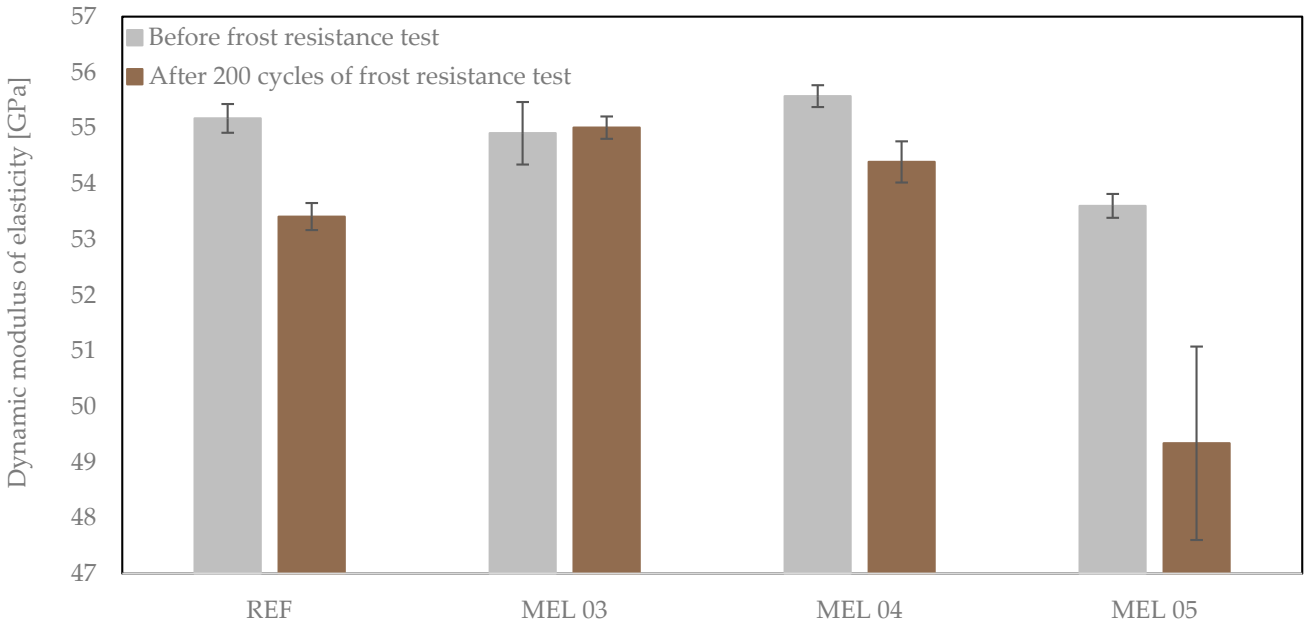


Figure 15. Comparison of the dynamic modulus of elasticity before and after the frost resistance test.

2.7. Frost Resistance

For the frost resistance test performed according to the ČSN 73 1322 standard [52], the same samples that had previously been subjected to the determination of the dynamic modulus of elasticity were used. The frost resistance coefficient was calculated based on the flexural strength of the reference and frozen samples according to the standard [52]. Table 4 provides the flexural strength values and frost resistance coefficients. The data for compressive and flexural strengths are graphically represented in Figure 16.

Table 4. Flexural strength before and after frost resistance testing with respective frost resistance coefficients.

Mixture	Average Flexural Strength before Frost Resistance Test [MPa]	Average Flexural Strength after 200 Cycles of Frost Resistance Test [MPa]	Frost Resistance Coefficient [%]
REF	14.3	14.6	102.3
MEL 03	14.1	14.5	102.5
MEL 04	15.4	15.5	100.1
MEL 05	11.4	11.2	97.7

The values in the graphs in Figure 16 show that the compressive and flexural strengths do not differ significantly from each other. Greater differences could be observed in the case of the REF and MEL 03 mixtures, which achieved slightly higher flexural strength values after frost resistance testing compared to the samples not subjected to this test. As for the MEL 05 mixture, there was a slight decrease in flexural strength after frost resistance testing (with significantly higher value dispersion in both cases). In any case, it seems that frost does not have such a significant destructive effect on high-quality concrete, and all mixtures are frost-resistant after 200 cycles according to the standard [52].

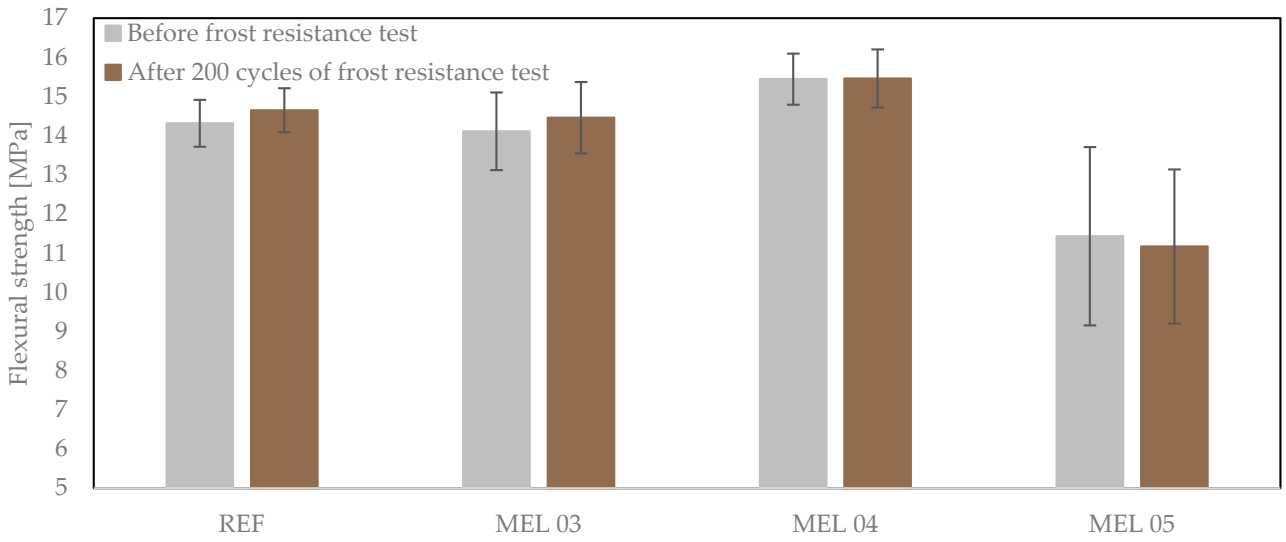


Figure 16. Comparison of flexural strength before and after the frost resistance test.

2.8. Load-Bearing Capacity of Reinforced Concrete Beams Made from Selected HPC Mixtures

For the purpose of load-bearing testing, two reinforced concrete beams were created, each with a length of 1150 mm and a cross-section of 100 × 190 mm, with one beam made from the reference mixture and the other from the MEL 04 mixture. The span during loading was 900 mm. During concreting, both beams were reinforced with a steel rebar reinforcement of 3 × ϕ 10 mm. The loading scheme is illustrated in Figure 17. The corresponding photographic documentation of the testing process is shown in Figure 18.

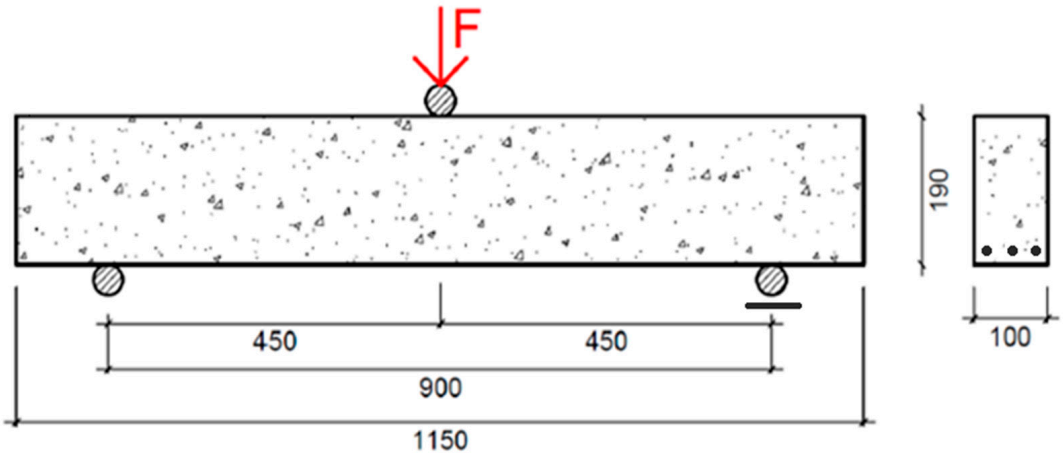


Figure 17. Load-bearing capacity test schema of reinforced concrete beam.

As shown in Figure 18, both beams exhibit shear cracks. In the case of the beam made from the MEL 04 mixture, the crack developed only on one side, whereas in the case of the beam made from the reference mixture, cracks appeared on both sides. No tensile cracks were developed in either case. The beam made from the reference mixture achieved the highest load-bearing capacity, reaching 78.5 kN, while the beam made from the MEL 04 mixture reached a maximum load-bearing capacity of 55 kN. The level of deformation was irrelevant in this case, as the loading was terminated without failure of the steel reinforcement. The loading process was also captured and evaluated in the form of a graph shown in Figure 19.



(**a**) (**b**)

Figure 18. Photos of the shear crack after the load-bearing capacity test of reinforced concrete beams made from the (**a**) REF and (**b**) MEL 04 mixtures.

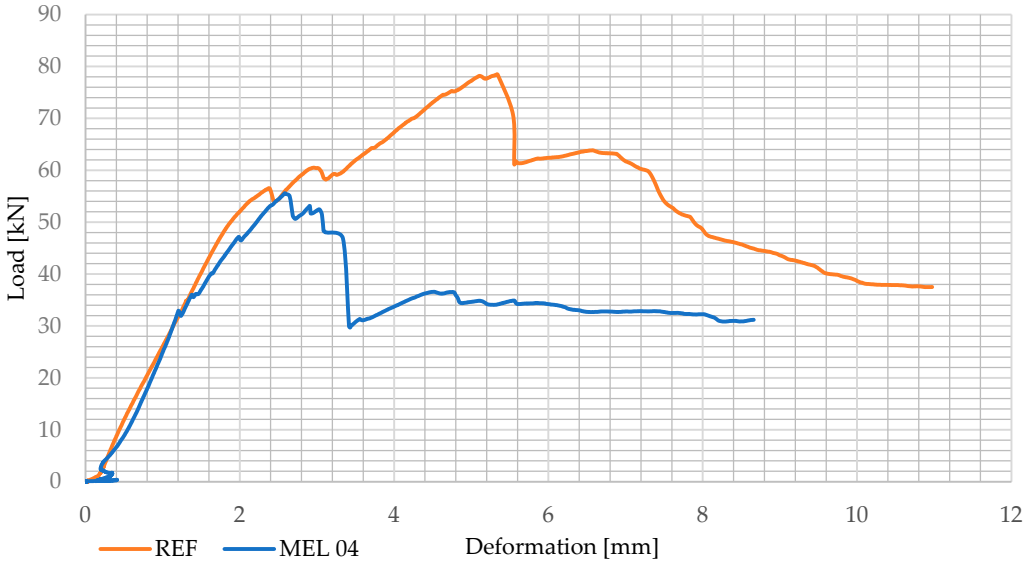


Figure 19. Load diagram of reinforced concrete beams made from the REF and MEL 04 mixtures.

3. Discussion

The presented study and experimental program [42] dealt with the topic of utilizing a dry mixture of high-quality concrete and the proposal of a recipe with all the necessary input raw materials (except water), which covers aspects of sustainable construction and circular economy for advanced technology when raw materials available in the Czech Republic are used.

The Introduction provides an overview of the current trends in the field, while the experimental section describes tests of (primarily) mechanical and durability properties of the hardened mixtures made from the proposed high-performance concrete with various dosages of the powdered plasticizer based on the polymerization product Glycol, as well as comparisons of these properties with a reference high-performance concrete containing liquid plasticizers based on polycarboxylate, polyphosphonate, and polyether carboxylate.

The mini-cone flow test of the fresh mixtures established that all mixtures with the powdered plasticizer showed a thixotropic consistency, while the reference mixture with liquid plasticizers achieved a viscous consistency. Nevertheless, it is necessary to specify the thixotropic behavior and determine the optimal thixotropic range in which the mixtures will print well, maintain their shape, and fluidize under dynamic disturbances.

Bulk density decreased almost directly proportionally with an increasing amount of powdered plasticizer due to the higher air content in the MEL mixtures, which could negatively affect the mechanical properties of the extruded 3D element.

The average 28-day compressive strength on cubes with a 100 mm edge length reached 122.9 MPa for the reference mixture, and the lowest value was obtained for the mixture with 5% powdered plasticizer (99.2 MPa). Regarding the compressive strength on 40 × 40 × 160 mm beam fragments, the reference mixture achieved a value approximately 3.5% lower than its cubic compressive strength. The MEL 03 and MEL 04 mixtures achieved values that were approximately 3.5% higher than their 28-day cubic compressive strength values. The MEL 04 mixture showed negligible differences in compressive strength. The dosage of powdered plasticizer significantly influenced the 7-day compressive strength. The reference mixture achieved approximately 93% of the 28-day compressive strength at this timepoint. In the presence of the powdered plasticizer, this strength noticeably decreased. For the mixture with a 5% content of powdered plasticizer, the 7-day compressive strength reached only about 25% of the 28-day strength. After 56 days, the compressive strength increased, on average, by 5.5% (MEL 03) up to 11.7% (MEL 05) compared to the 28-day strength.

Tensile splitting strength was tested on cube samples with a 150 mm edge length after 28 days from the day of concreting the samples. The values of the REF, MEL 03, and MEL 04 mixtures approached 7 MPa, while the MEL 05 mixture achieved a value of 6 MPa.

Flexural strength was tested on beam samples with dimensions of 40 × 40 × 160 mm within an interval of 7–56 days. Similar to compressive strength, the flexural strength of the reference mixture reached a high initial value (13 MPa), while the MEL 05 mixture achieved the lowest (3.8 MPa). However, after 56 days, all mixtures became relatively stabilized and reached values within the range of 14.1–14.9 MPa. For this test, as well as for the tensile splitting strength test, reinforced samples would be more relevant.

The problem sets in the initial days, when the powdered plasticizer probably limits the hydration of the mixture, which manifests itself in a "rubbery" and stickier structure of the samples and low strength characteristics. In the case of a 3D-extruded element, this could be a positive feature as the adhesion of the individual layers would increase. It is questionable to what extent the lower layers could withstand the load from the layers above them in the first days of ripening.

The test of resistance to water and defrosting chemicals showed the following results: the REF, MEL 03, and MEL 04 mixtures had relatively low waste after 200 cycles (all around 80–130 g/m^2); however, the MEL 05 mixture achieved significantly higher deterioration compared to the other mixtures, reaching 680 g/m^2 after 200 cycles. From the results, it is evident that the transition in the powdered plasticizer dosage between 4 and 5% is critical for resistance to water and defrosting chemicals.

The more porous structure of the mixture with a higher content of powdered plasticizer allowed for easier penetration of the NaCl solution into the structure of the samples, which led to faster breakage of the samples by the defrosting chemicals. It is important to realize that 3D-printed concrete is still in the early stages of development, and several more acute problems need to be solved before it can be applied in environments with increased exposure to water and chemical defrosting agents.

The frost resistance of the tested samples demonstrated the high durability of all mixtures, with the lowest values for the MEL 05 mixture, whose frost resistance coefficient after 200 cycles reached 97.7%.

The ultrasonic pulse method revealed negligible changes in the dynamic modulus of elasticity after the frost resistance test compared to the reference 28-day samples for all mixtures. In the case of the MEL 05 mixture, this change was most evident; after the frost resistance test, there was a decrease in the dynamic modulus of elasticity by approximately 7.5%. This was caused again by a more porous structure. In this case, the ability to withstand dynamic loads remained almost unchanged for most of the tested mixtures. The

determination of the static modulus of elasticity appears to be a suitable complement to verifying the material characteristics of the researched mixtures.

In the end, the REF and MEL 04 mixtures were compared for their load-bearing capacity using reinforced concrete beams with dimensions of 100 × 190 × 1150 mm and a span of 900 mm; these concrete beams were reinforced with three steel bars with a diameter of 10 mm at the bottom edge. The reference mixture achieved approximately 40% higher load-bearing capacity (78.5 kN) than the MEL 03 mixture (55 kN). In both cases, a shear crack was identified after reaching the maximum load. The test demonstrated the loading of the beams in simple bending without the use of shear reinforcement. This type of beam is less demanding from a technological and financial perspective but has limited application compared to structural elements supplemented with shear reinforcement. Although the testing of this type of structural element is not directly related to 3D printing technology, it was included in the experimental program to understand the cointegration with concrete reinforcement.

4. Conclusions

A series of strength tests, including compressive, flexural, and splitting tensile strength tests, were carried out on beam samples with dimensions of 40 × 40 × 160 mm and cubes with lengths of 100 and 150 mm. In addition, durability tests were carried out, namely, resistance to water, defrosting chemicals, and frost tests. In the case of frost resistance, the change in the dynamic modulus of elasticity was monitored and compared with that of samples not subjected to cyclic freezing and thawing. Finally, the load-bearing capacity of the reinforced beams with dimensions of 100 × 190 × 1150 mm made from the REF and MEL 04 mixtures was tested. A summary [42] of these tests is presented below:

- Bulk density increased with increasing plasticizer content due to the formation of a more porous structure.
- The highest cube compressive strength after 28 days was achieved for the MEL 03 mixture at 121.6 MPa, and the lowest was achieved for the MEL 05 mixture at 102.8 MPa. The highest tensile splitting strength was achieved for the REF mixture at 6.91 MPa, and the lowest was achieved for the MEL 05 mixture at 5.99 MPa.
- The MEL 05 mixture reached the lowest 7-day compression strength at 24.76 MPa and flexure strength at 3.8 MPa.
- The results of the strength characteristics show that a powdered plasticizer content above 5% significantly slows down the setting and hardening time of the mixtures in the early stages of maturation.
- The REF, MEL 03, and MEL 04 mixtures achieved a relatively low waste amount after 200 cycles of testing for resistance to water and defrosting chemicals, at approx. 80–130 g/m^2. The MEL 05 mixture achieved a waste amount of 680 g/m^2 after 200 cycles due to its more porous structure. All mixtures were also frost-resistant after 200 cycles of cyclic freezing and thawing.

The creation of dry-mixed, high-performance concrete for advanced manufacturing technologies is a non-negligible factor in terms of reducing labor costs. In addition to testing hardened samples, further research needs to focus on fresh mixtures. The present research focused only on the behavior of hardened mixtures. The rheological properties of fresh mixtures, essential for the proper design of mixtures suitable for advanced manufacturing technologies, were not the subject of this study, nor was testing on 3D-printed specimens. In future studies, it is therefore necessary to establish a correlation between the tested mixtures and these characteristics. Further research will be devoted to the use of advanced additive printing technology and printing solutions, where it is expected to be used for solutions with higher added value and design aspects as part of an innovative technological printing solution for silicate materials.

Author Contributions: Conceptualization, O.S.; methodology, V.B.; validation, R.G.; formal analysis, P.C.; investigation, P.C.; resources, P.C.; data curation, P.C., R.G. and J.J.; writing—original draft preparation, R.G. and P.C.; writing—rewrite O.S.; visualization, J.J.; supervision, V.B.; project administration, O.S. All authors have read and agreed to the published version of the manuscript.

Funding: This research was funded by the Jan Amos Komensky Operational Program, financed by the European Union and the state budget of the Czech Republic (grant number CZ.02.01.01/00/22_008/0004631 (Materials and technologies for sustainable development)). This research also received support from the Ministry of Education, specifically from the Student Research Grant Competition of the Technical University of Ostrava under identification number SP2024/072.

Data Availability Statement: The data presented in this study are available on Zenodo, https://zenodo.org/records/10940667.

Acknowledgments: This paper was written as part of project no. CZ.02.01.01/00/22_008/0004631 (Materials and technologies for sustainable development) within the Jan Amos Komensky Operational Program financed by the European Union and the state budget of the Czech Republic. This research also received support from the Ministry of Education, specifically from the Student Research Grant Competition of the Technical University of Ostrava under identification number SP2024/072.

Conflicts of Interest: The authors declare no conflicts of interest.

References

1. Buswell, R.A.; Leal de Silva, W.R.; Jones, S.Z.; Dirrenberger, J. 3D Printing Using Concrete Extrusion: A Roadmap for Research. *Cem. Concr. Res.* **2018**, *112*, 37–49. [CrossRef]
2. Wolfs, R.J.M.; Bos, F.P.; Salet, T.A.M. Early Age Mechanical Behaviour of 3D Printed Concrete: Numerical Modelling and Experimental Testing. *Cem. Concr. Res.* **2018**, *106*, 103–116. [CrossRef]
3. Lim, J.H.; Weng, Y.; Pham, Q.-C. 3D Printing of Curved Concrete Surfaces Using Adaptable Membrane Formwork. *Constr. Build. Mater.* **2020**, *232*, 117075. [CrossRef]
4. Zhang, C.; Nerella, V.N.; Krishna, A.; Wang, S.; Zhang, Y.; Mechtcherine, V.; Banthia, N. Mix Design Concepts for 3D Printable Concrete: A Review. *Cem. Concr. Compos.* **2021**, *122*, 104155. [CrossRef]
5. Menna, C.; Mata-Falcón, J.; Bos, F.P.; Vantyghem, G.; Ferrara, L.; Asprone, D.; Salet, T.; Kaufmann, W. Opportunities and Challenges for Structural Engineering of Digitally Fabricated Concrete. *Cem. Concr. Res.* **2020**, *133*, 106079. [CrossRef]
6. Khan, M.S.; Sanchez, F.; Zhou, H. 3-D Printing of Concrete: Beyond Horizons. *Cem. Concr. Res.* **2020**, *133*, 106070. [CrossRef]
7. Ngo, T.D.; Kashani, A.; Imbalzano, G.; Nguyen, K.T.Q.; Hui, D. Additive Manufacturing (3D Printing): A Review of Materials, Methods, Applications and Challenges. *Compos. Part B Eng.* **2018**, *143*, 172–196. [CrossRef]
8. Quah, T.K.N.; Tay, Y.W.D.; Lim, J.H.; Tan, M.J.; Wong, T.N.; Li, K.H.H. Concrete 3D Printing: Process Parameters for Process Control, Monitoring and Diagnosis in Automation and Construction. *Mathematics* **2023**, *11*, 1499. [CrossRef]
9. Zhang, J.; Wang, J.; Dong, S.; Yu, X.; Han, B. A Review of the Current Progress and Application of 3D Printed Concrete. *Compos. Part A Appl. Sci. Manuf.* **2019**, *125*, 105533. [CrossRef]
10. Wu, P.; Wang, J.; Wang, X. A Critical Review of the Use of 3-D Printing in the Construction Industry. *Autom. Constr.* **2016**, *68*, 21–31. [CrossRef]
11. Bhooshan, S.; Bhooshan, V.; Dell'Endice, A.; Chu, J.; Singer, P.; Megens, J.; Van Mele, T.; Block, P. The Striatus Bridge: Computational design and robotic fabrication of an unreinforced, 3D-concrete-printed, masonry arch bridge. *Archit. Struct. Constr.* **2022**, *2*, 521–543. [CrossRef]
12. Weger, D.; Gehlen, C.; Korte, W.; Meyer-Brötz, F.; Scheydt, J.; Stengel, T. Building Rethought–3D Concrete Printing in Building Practice. *Constr. Robot.* **2021**, *5*, 203–210. [CrossRef]
13. Salandin, A.; Quintana-Gallardo, A.; Gómez-Lozano, V.; Guillén-Guillamón, I. The First 3D-Printed Building in Spain: A Study on Its Acoustic, Thermal and Environmental Performance. *Sustainability* **2022**, *14*, 13204. [CrossRef]
14. Nováková, K.; Vele, J.; Litoš, J.; Šána, V. Prvok-Issue on 3D Printing Concrete Building. *Acta Polytech. CTU Proc.* **2022**, *38*, 247–254. [CrossRef]
15. Elantary, A.; Aldubaisi, F.; Abahussain, S.; Alasif, Z. Creating A 3D Printed Residential Building in Qatif. *Umm Al-Qura Univ. J. Eng. Archit.* **2021**, *1*, 8–13.
16. Shen, W.; Cao, L.; Li, Q.; Zhang, W.; Wang, G.; Li, C. Quantifying CO_2 Emissions from China's Cement Industry. *Renew. Sustain. Energy Rev.* **2015**, *50*, 1004–1012. [CrossRef]
17. Hanifa, M.; Agarwal, R.; Sharma, U.; Thapliyal, P.C.; Singh, L.P. A Review on CO_2 Capture and Sequestration in the Construction Industry: Emerging Approaches and Commercialised Technologies. *J. CO2 Util.* **2023**, *67*, 102292. [CrossRef]
18. Tay, Y.W.D.; Panda, B.N.; Ting, G.H.A.; Ahamed, N.M.N.; Tan, M.J.; Chua, C.K. 3D Printing for Sustainable Construction. In *Industry 4.0–Shaping the Future of the Digital World*; CRC Press: Boca Raton, FL, USA, 2020; pp. 119–123. [CrossRef]
19. Lediga, R.; Kruger, D. Optimizing Concrete Mix Design for Application in 3D Printing Technology for the Construction Industry. *Solid State Phenom.* **2017**, *263*, 24–29. [CrossRef]

20. Tabassum, T.; Ahmad Mir, A. A Review of 3d Printing Technology-the Future of Sustainable Construction. *Mater. Today Proc.* **2023**, *93*, 408–414. [CrossRef]
21. Xiao, C.; Zheng, K.; Chen, S.; Li, N.; Shang, X.; Wang, F.; Liang, J.; Khan, S.B.; Shen, Y.; Lu, B.; et al. Additive manufacturing of high solid content lunar regolith simulant paste based on vat photopolymerization and the effect of water addition on paste retention properties, *Addit. Manuf.* **2023**, *71*, 103607. [CrossRef]
22. Mateckova, P.; Bilek, V.; Sucharda, O. Comparative Study of High-Performance Concrete Characteristics and Loading Test of Pretensioned Experimental Beams. *Crystals* **2021**, *11*, 427. [CrossRef]
23. Huang, H.; Yuan, Y.; Zhang, W.; Zhu, L. Property Assessment of High-Performance Concrete Containing Three Types of Fibers. *Int. J. Concr. Struct. Mater.* **2021**, *15*, 1–17. [CrossRef]
24. Sucharda, O.; Marcalikova, Z.; Gandel, R. Microstructure, Shrinkage, and Mechanical Properties of Concrete with Fibers and Experiments of Reinforced Concrete Beams without Shear Reinforcement. *Materials* **2022**, *15*, 5707. [CrossRef]
25. Marcalikova, Z.; Jerabek, J.; Gandel, R.; Gabor, R.; Bilek, V.; Sucharda, O. Mechanical Properties, Workability, and Experiments of Reinforced Composite Beams with Alternative Binder and Aggregate. *Buildings* **2024**, *14*, 2142. [CrossRef]
26. Fernández-Jiménez, A.; Palomo, A. Composition and Microstructure of Alkali Activated Fly Ash Binder: Effect of the Activator. *Cem. Concr. Res.* **2005**, *35*, 1984–1992. [CrossRef]
27. Šimonová, H.; Kucharczyková, B.; Bílek, V.; Malíková, L.; Miarka, P.; Lipowczan, M. Mechanical Fracture and Fatigue Characteristics of Fine-Grained Composite Based on Sodium Hydroxide-Activated Slag Cured under High Relative Humidity. *Appl. Sci.* **2020**, *11*, 259. [CrossRef]
28. Gandel, R.; Jerabek, J.; Marcalikova, Z. Reinforced Concrete Beams Without Shear Reinforcement Using Fiber Reinforced Concrete and Alkali-Activated Material. *Civ. Environ. Eng.* **2023**, *19*, 348–356. [CrossRef]
29. Yao, X.; Lyu, X.; Sun, J.; Wang, B.; Wang, Y.; Yang, M.; Wei, Y.; Elchalakani, M.; Li, D.; Wang, X. AI-based performance prediction for 3D-printed concrete considering anisotropy and steam curing condition, *Constr. Build. Mater.* **2023**, *375*, 130898. [CrossRef]
30. Gökçe, H.S.; Tuyan, M.; Nehdi, M.L. Alkali-Activated and Geopolymer Materials Developed Using Innovative Manufacturing Techniques: A Critical Review. *Constr. Build. Mater.* **2021**, *303*, 124483. [CrossRef]
31. Qaidi, S.; Yahia, A.; Tayeh, B.A.; Unis, H.; Faraj, R.; Mohammed, A. 3D Printed Geopolymer Composites: A Review. *Mater. Today Sustain.* **2022**, *20*, 100240. [CrossRef]
32. Mengistu, G.M.; Nemes, R. Recycling 3D Printed Concrete Waste for Normal Strength Concrete Production. *Appl. Sci.* **2024**, *14*, 1142. [CrossRef]
33. Ungureanu, D.; Onuțu, C.; Isopescu, D.N.; Țăranu, N.; Zghibarcea, Ș.V.; Spiridon, I.A.; Polcovnicu, R.A. A Novel Approach for 3D Printing Fiber-Reinforced Mortars. *Materials* **2023**, *16*, 4609. [CrossRef] [PubMed]
34. Li, Y.-F.; Tsai, P.-J.; Syu, J.-Y.; Lok, M.-H.; Chen, H.-S. Mechanical Properties of 3D-Printed Carbon Fiber-Reinforced Cement Mortar. *Fibers* **2023**, *11*, 109. [CrossRef]
35. Arunothayan, A.R.; Nematollahi, B.; Ranade, R.; Bong, S.H.; Sanjayan, J. Development of 3D-Printable Ultra-High Performance Fiber-Reinforced Concrete for Digital Construction. *Constr. Build. Mater.* **2020**, *257*, 119546. [CrossRef]
36. Bai, G.; Chen, G.; Li, R.; Wang, L.; Ma, G. 3D Printed Ultra-High Performance Concrete: Preparation, Application, and Challenges. In *Lecture Notes in Civil Engineering*; Springer: Singapore, 2023; pp. 53–65. [CrossRef]
37. Arunothayan, A.R.; Nematollahi, B.; Khayat, K.H.; Ramesh, A.; Sanjayan, J.G. Rheological Characterization of Ultra-High Performance Concrete for 3D Printing. *Cem. Concr. Compos.* **2023**, *136*, 104854. [CrossRef]
38. Kaszyńska, M.; Hoffmann, M.; Skibicki, S.; Zieliński, A.; Techman, M.; Olczyk, N.; Wróblewski, T. Evaluation of Suitability for 3D Printing of High Performance Concretes. *MATEC Web Conf.* **2018**, *163*, 01002. [CrossRef]
39. Le, T.T.; Austin, S.A.; Lim, S.; Buswell, R.A.; Gibb, A.G.F.; Thorpe, T. Mix design and fresh properties for high-performance printing concrete, *Mater. Struct.* **2012**, *45*, 1221–1232. [CrossRef]
40. Wolfs, R.J.M.; Bos, F.P.; Salet, T.A.M. Hardened properties of 3D printed concrete: The influence of process parameters on interlayer adhesion, *Cem. Concr. Res.* **2019**, *119*, 132–140. [CrossRef]
41. Sanjayan, J.G.; Nematollahi, B.; Xia, M.; Marchment, T. Effect of surface moisture on inter-layer strength of 3D printed concrete, *Constr. Build. Mater.* **2018**, *172*, 468–475. [CrossRef]
42. Sucharda, O.; Gandel, R.; Ćmiel, P.; Jeřábek, J.; Bílek, V. Utilization of High-Performance Concrete Mixtures for Advanced Manufacturing Technologies—Experimental Dataset. 2024. Available online: https://zenodo.org/records/10940667 (accessed on 5 April 2024).
43. Ćmiel, P. Properties of Concrete and Development of Concrete Formulas for Advanced and Additive Technologies. Master's thesis, VSB–Technical University of Ostrava, Ostrava, Czechia, 2023.
44. *ČSN EN 1015-3*; Methods of Test for Mortar for Masonry—Part 3: Determination of Consistence of Fresh Mortar (by Flow Table). Czech Institute for Standardization: Prague, Czech Republic, 2000.
45. Robert, C.; Kalný, M.; Kolísko, J.; Vítek, J.L. *Ultra-high-performance concrete (TP ČBS 07 Vysokohodnotný Beton-UHPC)*; ČBS—Czech Concrete Society: Praha, Czech Republic, 2022.
46. *ČSN EN 12390-3*; Testing Hardened Concrete—Part 3: Compressive Strength of Test Specimens. Czech Standardization Agency: Prague, Czech Republic, 2020.
47. *ČSN EN 196-1*; Methods of Testing Cement—Part 1: Determination of Strength. Czech Office for Standards, Metrology and Testing: Prague, Czech Republic, 2016.

48. *ČSN EN 12390-6*; Testing Hardened Concrete—Part 6: Tensile Splitting Strength of Test Specimens. Czech Office for Standards, Metrology and Testing: Prague, Czech Republic, 2024.
49. *ČSN EN 12390-5*; Testing Hardened Concrete—Part 5: Flexural Strength of Test Specimens. Czech Office for Standards, Metrology and Testing: Prague, Czech Republic, 2020.
50. *ČSN 73 1326*; Resistance of Cement Concrete Surface to Water and Defrosting Chemicals. Czech Standardization Agency: Prague, Czech Republic, 1984.
51. *ČSN 73 1371*; Non-Destructive Testing of Concrete—Method of Ultrasonic Pulse Testing of Concrete. Czech Office for Standards, Metrology and Testing: Prague, Czech Republic, 2011.
52. *ČSN 73 1322*; Determination of Frost Resistance of Concrete. Czech Standardization Agency: Prague, Czech Republic, 1968.

Disclaimer/Publisher's Note: The statements, opinions and data contained in all publications are solely those of the individual author(s) and contributor(s) and not of MDPI and/or the editor(s). MDPI and/or the editor(s) disclaim responsibility for any injury to people or property resulting from any ideas, methods, instructions or products referred to in the content.